Collagen and Leather

COMMUNICATION

Open Access

Spider-capture-silk mimicking fibers with high-performance fog collection derived from superhydrophilicity and volume-swelling of gelatin knots

Yuanzhang Jiang[1], Harun Venkatesan[2], Shuo Shi[3], Cong Wang[3], Miao Cui[4,5], Qiang Zhang[1], Lin Tan[1,6*] and Jinlian Hu[3,7*]

Abstract

Spider-capture-silk (SCS) can directionally capture and transport water from humid air relying on the unique geometrical structure. Although there have been adequate reports on the fabrication of artificial SCSs from petroleum-based materials, it remains a big challenge to innovate bio-based SCS mimicking fibers with high-performance fog collection ability and efficiency simultaneously. Herein, we report an eco-friendly and economical fiber system for water collection by coating gelatin on degummed silk. Compared to the previously reported fibers with the best fog collection ability (~ 13.10 μL), Gelatin on silk fiber 10 (GSF10) can collect larger water droplet (~ 16.70 μL in 330 s) with ~ 98% less mass. Meanwhile, the water collection efficiency of GSF10 demonstrates ~ 72% and ~ 48% enhancement to the existing best water collection polymer coated SCS fibers and spidroin eMaSp2 coated degummed silk respectively in terms of volume-to-TCL (vapor–liquid-solid three-phase contact line) index. The simultaneous function of superhydrophilicity, surface energy gradient, and ~ 65% water-induced volume swelling of the gelatin knots are the key factors in advancing the water collection performance. Abundant availability of feedstocks and ~ 75% improved space utilization guarantee the scalability and practical application of such bio-based fiber.

Keywords Artificial spider-capture-silk, Directional water collection, Volume-to-TCL index, Superhydrophilicity, Volume swelling

*Correspondence:
Lin Tan
tanlinou@scu.edu.cn
Jinlian Hu
jinliahu@cityu.edu.hk
Full list of author information is available at the end of the article

Graphic Abstract

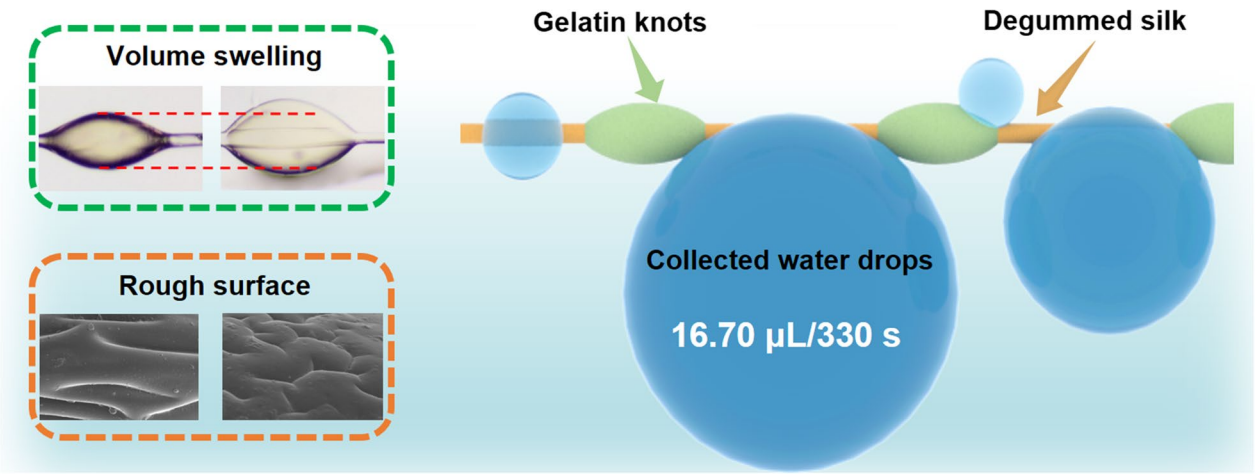

1 Introduction

As a type of sustainable fresh water, fog can be collected to alleviate the severe water scarcity occurring in many areas caused by climate change, population growth and pollution [1–4]. In arid regions, some creatures have evolved the ability to harvest fog through special chemical or physical methods to survive the extreme environment [5, 6]. For example, some types of beetles live in *Namib Desert* can harvest water from the morning mist utilizing their patterned backs [7, 8]. In Australia, green tree frogs and desert lizards can collect dews through their superhydrophobic/superhydrophilic skin [9, 10]. Moreover, spiders can produce web with the periodic spindle knots constructed by nanofibrils on SCS enable the directional water collection and transportation from humid air [11–14]. Particularly, spider silks have attracted world-wide intensive studies due to its fabulous properties and hierarchical structures.

The very first report on the discovery of the relationship between the silk structure and directional water collection was demonstrated via Jiang et al. in 2010. They found that the structure induced synergy of surface energy and curvature gradient endowed the directional water collection of SCS [12]. Afterwards, a series of SCS mimicking fibers were fabricated by coating different polymers [Poly(vinyl alcohol) (PVA), Polymethyl methacrylate (PMMA), Polystyrene (PS), Polyvinylidene difluoride (PVDF)] on various fibers (Nylon fiber, copper wire, and fishing line) to achieve the "spindle knots/joints" construction of SCS through various approaches like dip-coating, electrospinning and microfluidic spinning [15–22]. However, most of the artificial SCS modified with non-renewable fossil resources have a hydrophobic shell which decreases their sensitivity to water. Furthermore, the utilization of undegradable polymers deriving from non-renewable fossil resources by traditional methods will accelerate the seepd of energy depletion and may result in severe environmental pollution. To address these problems, in our previous report, we created SCS like fibers that exhibited fabulous water collection efficiency by coating transgenetic spider dragline protein (eMaSp2) on degummed cocoon silk [23]. Nevertheless, the spidroin material obtained by gene bioengineering suffers form low yield and high cost. As an alternation of eMaSp2, gelatin, which is widely existing in nature, is an economic and affordable candidate for SCS modification beacuse of the similarity to spidroin [24, 25]. First, both of them are constructed via amino acids. The glue like spidroin ASG2 is mainly comprised of Serine, Glycine and Valine, and gelatin is rich in Glycine, Valine, Proline and Hydroxyproline [26]. Second, they are both hydrophilic biomaterials. Gelatin is often used as a matrix material for face mask and hydrophilic drug carrier, and the viscid glue coated on spider spiral silk demonstrated excellent adhesive in wet/dry conditions, which could be ascribed to their hydrophilicity [27, 28]. Therefore, gelatin would be an ideal substitute of the eMaSp2.

In the present paper, as sketched in Fig. 1, a series of SCS inspired fibers were fabricated by coating porcine gelatin on degummed silkworm silk through a facile dip-coating process following by a cross-linking in Glutaraldehyde steam. Morphology observation indicated the construction of periodic spindle knots on the fiber surface. Water contact angle test revealed that gelatin could

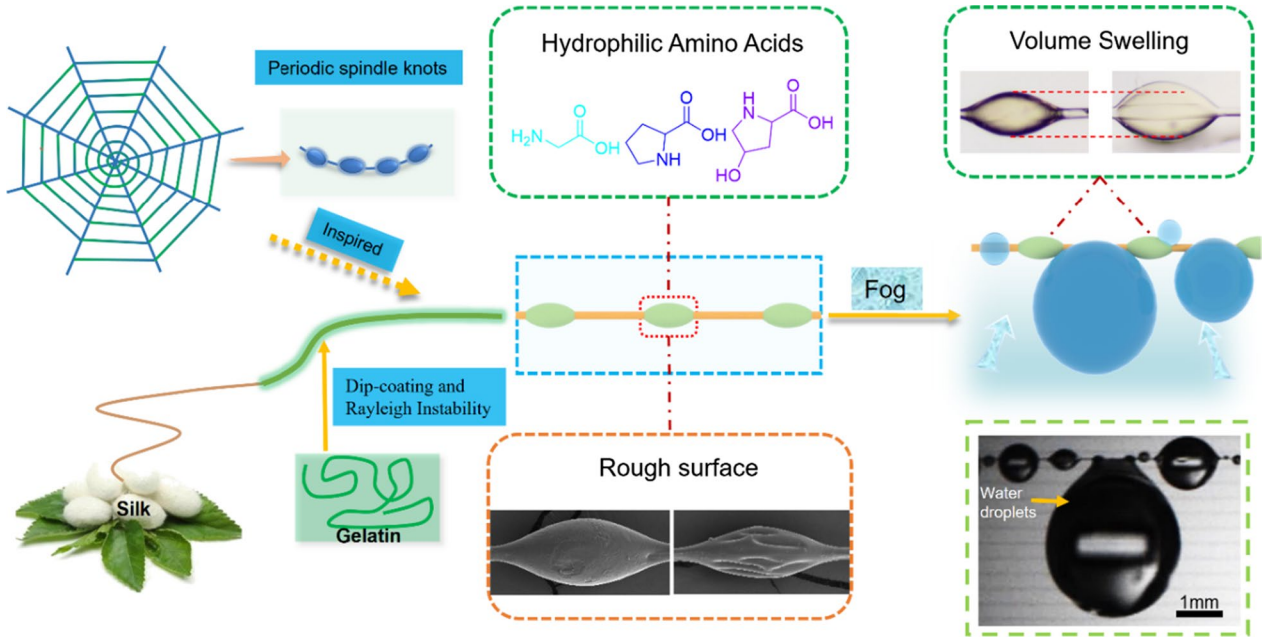

Fig. 1 Schematic illustration of the preparation and fog collection ability of GSF

become superhydrophilic within 6 min. Meanwhile, in the fog collection experiment, we found that the collected water could swell the spindle knots and result in increasing the knot volume, vapor–liquid-solid three-phase contact line (TCL) and the curvature value of the SCS fibers simultaneously. These factors led to the high speed and large volume directional fog collection capability (~ 16.70 μL water per repeat unit of spindle knot in 330 s). To the best of our knowledge, this economical and sustainable SCS modificaiton system with high-performance directional water collection ability is reported for the first time.

2 Materials and methods

2.1 Materials

Gelatin from porcine skin (gel strength ~ 300 g Bloom) was supplied by Sigma-Aldrich. 1, 1, 1, 3, 3, 3-hexafluoroisopropanol (HFIP) was received from J & K Scientific Ltd. *B. Mori* silk cocoons were purchased from Taobao. Na_2CO_3 and Glutaraldehyde, 25 wt% solution in H_2O were puechased from Kelong Chemical Regent Co., Ltd. (Chengdu, China). All materials were used without further treatment.

2.2 Preparation of degummed silk

The degum process of silkworm silk was conducted according to previous report [29]. Generally, *B. Mori* cocoons were cut into small pieces and then boiled in 0.02 M Na_2CO_3 for 30 min. The silk was subsequentially rinsed by ultrapure water for three times and dried in fume hood for 24 h. The dried silk was separated into single fibers before use.

2.3 Preparation of gelatin/HFIP solution

Gelatin powder was put in flasks with a stir bar. And then HFIP was added to dissolve gelatin powder and give the solution at 8%, 10% and 12% concentrations, respectively.

2.4 Fabrication of artificial SCS fibers

A facile dip-coating strategy was applied to fabricated fibers with periodic spindle knots based our previous report. Typically, one degummed silk fiber was first horizontally soaked in gelatin/HFIP solution and drawn out steadily, following by the break up process of the thin film coated on fiber surface and appearance of little drops resulted from the Rayleigh Instability. After drying in air for 30 min, the fiber was exposed in Glutaraldehyde steam in a glass desiccator for 10 min for cross linking. Subsequently, the fiber with periodic spindle knots was wash by ultrapure water and dried in a fume hood.

2.5 Fabrication of gelatin films and degummed silk fibrion films for water contact angle test

Gelatin/HFIP was poured into Teflon molds and dried at room temperature to give gelatin films. For degummed silk fibroin films, the degummed silk was dissolved in

HFIP at 50 °C for 3 days, and then the solution was poured into Teflon molds and dried at room temperature.

2.6 Charactrization

The morphology of GSF fibers was observed by Scanning electron microscopy (SEM, Apreo S HiVoc, USA) and a contact angle tester (Harke-SPCAX1, China). Fourier transform infrared (FTIR) spectra were obtained using a IRTracer-100 spectrometer (Shimadzu, Japan). Mechanical properties of the fibers were investigated by a fiber tensile tester (YM061FQ-120, China).

2.7 Water collection observation and analysis

Degummed silk and GSF fibers were hold by two retort stands with extension clamps. An ultrasonic humidifier was employed to supply the fog environment and the humidity around the fiber was ~ 95% tested by a Digital Thermometer Humidity Meter (PEAKMETER-PM6508). A contact angle tester (Harke-SPCAX1, China) with digital camera was applied to observe the water collection. Photos were taken by the camera connected to the Harke-SPCAX1, and analyzed by Image J. And the videos were recorded by a screen recording software (Bandicam). The volume of droplets was calculated according to reported formula $\frac{4}{3}\pi r_a^2 r_b$, where r_a and r_b are the width and height of the droplets. The purity of the collected water was evaluated by testing the ohmic value obtained by a multimeter at constant distance between the electrodes.

2.8 Water contact angle (CA) test

The CAs of gelatin films and silk films were measured through a contact angle tester (Harke-SPCAX1, China). At least five individual values were collected and averaged. A water droplet of 15 μL was used as the indicator.

2.9 Swelling and shrinkage observation of gelatin spindle knot

The swelling and shrinking of gelatin knots were observed and recorded by a microscope with a digital camera (Phinex PH-100, China). For the swelling test, fiber was gently put on a glass slide and little water was injected by a micro syringe to immerse the knot and trigger the swelling. For shrinkage, the water around the knot was sucked away by absorbent paper and then the knot started to shrink due to the continuous evaporation of water.

3 Results and discussion

3.1 Characterization of GSF

The well distributed periodic spindle knots of the SCS mimicking fiber is the key to achieve the high fog harvesting efficiency and ability. Figure 1 sketched a simple dip-coating fabrication strategy applied in this study. Gelatin derived from porcine skin was dissolved in HFIP to give gelatin/HFIP coating solution with different concentrations. Then, a degummed silkworm silk was soaked into the gelatin/HFIP solution and drawn out carefully. Due to the Rayleigh instability, the gelatin solution coating layer will break up and result in the periodic spindle knots. After exposure in Glutaraldehyde steam, the final fibers with periodic spindle cross-linked gelatin knots were obtained. Under different solution concentration conditions, the as-fabricated fibers showed various morphology. As illustrated in Additional file 1: Fig. S1, at low concentration (8 wt%), the size of the spindle knots was small and meanwhile the break-up process was found unsatisfactory because the diameter of the "joints part" silk fiber was observed enlarged to ~ 15 mm. Whereas, at high concentration (12 wt%), the volume of the spindle knots increased obviously accompanying the thicker fibers. Optimal fibers were prepared by coating 10 wt% gelatin/HFIP solution on silkworm silks. From the optical image (Fig. 2a) we found that this moderate concentration could not only facilitate the break-up of the cylindric liquid film on the silk surface but assist the formation of the periodic spindle knots as well. Scanning electron microscope (SEM) photos revealed that two types of surface topography were constructed by the macromolecular self-assemble of gelatin. As illustrated in in Fig. 2b, the nano-size wrinkled structure was observed on the surface of the round spindle knot, which is the major topography of the knots. Another typical morphology appeared on minor knots was shown in Fig. 2c. The fast evaporation of the solvent induced these ridge and valley structures on the knots. Besides, higher magnification photos displayed that the sub-micron cracks spread all over the knots' surface. These rough surface of the two types of spindle knots can magnify the pinning effect to TCL, which will help speed up the moisture accumulation and the water-hanging capability of the fibers [30].

FTIR was appplied to investigate the composition of GSF10. As shown in Additional file 1: Fig. S2, both degummed silk and GSF10 exhibited amid I peaks at 1616 cm^{-1}, which are corresponding to carbonyl (C=O) streching vibration from β-sheet. And amide II peaks at 1510 cm^{-1} can be assigned to N–H bending and C–N stretching. The peaks at 1265 and 1226 cm^{-1} (amide III band) was assigned to the β-sheet conformation. Moreover, after coated by gelatin, GSF10 presented a new peak at 2883 cm^{-1}, which can be ascribed to amide A of gelatin [31]. The mechanical property of the fibers is an important factor for the practical application. Therefore, tensile tests were conducted on degummed silk and various GSF10 and the results were sumarrized in Fig. 3. It is clear that after dip-coating, both the tensile stress and strain increased dramatically. The tensile stress increased

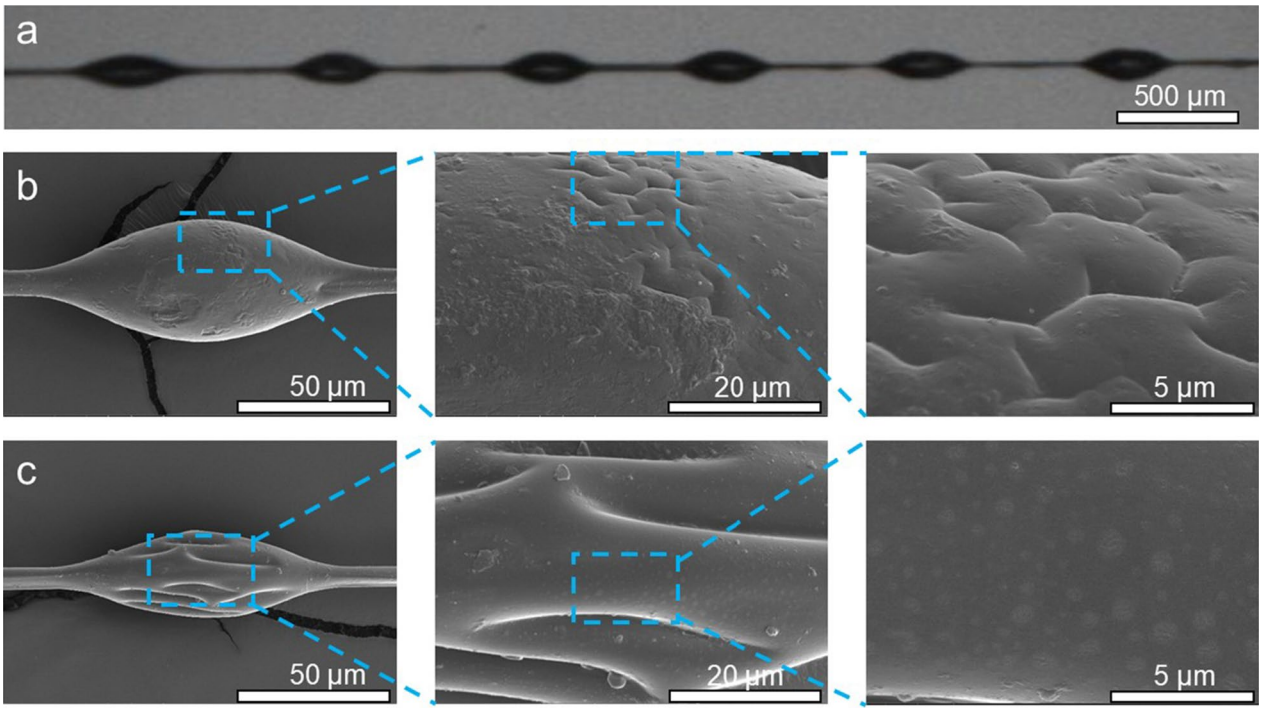

Fig. 2 The morphology of the fabricated fiber. **a** Optical image of GSF10. **b** and **c** Two types of SEM images of GSF10

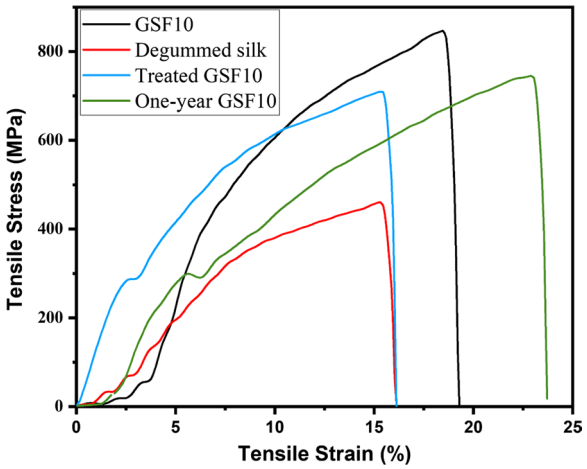

Fig. 3 Stress–strain curves of degummed fibers and various GSF10 (Treated GSF10: GSF10 that had been stored in a constant temperature and humidity chamber at 40 degrees and 30% humidity for 15 days; One-year GSF10: GSF10 that had been stored for around one year)

from 466.2 to 852.2 MPa, and the tensile strain increased from 16.1 to 19.2%. After being stored in at 40 degrees and 30% humidity for 15 days, compared to fresh-made GSF10, tensile stress of the treated ones decreased slightly from 852.2 to 752.9 MPa, but the tensile strain increased from 19.2 to 23.7%. Generally, the mechanical properties and durability of GSF10 were relatively stable in high temperature and low humidity conditions over a period of time. More importantly, after around one year of indoor storage, the tensile stress decreased from around 852.2 to 717.2 MPa, and the tensile strain also decreased from 19.2 to 16.5%. These indicate that as biomass-based material, the mechanical properties of GSF10 did decrease with time. However, this weakening is not significant and is within acceptable range.These indicate that GSF10 obtained good mechanical property that can be stored for a relative long time, which will help to increase the lifetime of the device in practical use.

3.2 Fog collection property

The water angle test instrument with a camera that can observe the in-situ water condensation process was applied to evaluate the water uptaking ability of the fibers. As shown in Fig. 4, compared with the original degummed silk, the fibers coated by 8 and 10 wt% gelatin solution, namely GSF8 and GSF10, displayed much enhanced fog collection ability by sustaining quite bigger droplets. To our surprise, quantitive analysis elucidated that the maximum droplets holding by two knots of GSF10 was calculated to be ~ 16.70 ± 1.32 μL, which was more than two times of the droplets volume collected by GSF8 (~ 5.14 ± 0.47 μL). By contrast, the ultimate volume of drops collected bare degummed silk was only ~ 2.53 ± 0.16 μL, which was consistent with our previous report [23]. On the other hand, due to the fabulous

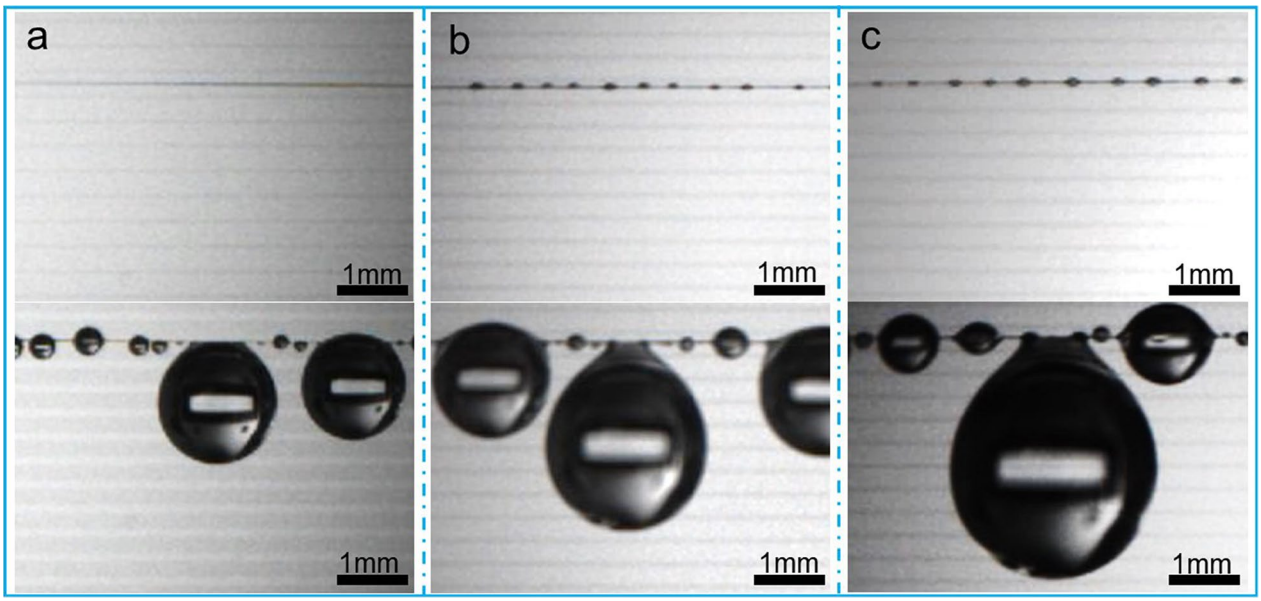

Fig. 4 Digital photos show the largest water droplets could be collected by different fibers under ~ 95% RH. **a** Degummed silk. **b** GSF8. **c** GSF10

water collection performance, the droplets collected by GSF10 were large enough to be pipetted and weighed by a high-precision analytical balance. The weight was measured to be ~ 13.02 ± 0.26 μg, similar to the result of the volume calculation. The reason why the former value is smaller may be due to the volatilization of water during weighing since the balance is fixed in another room. Intriguingly, by comparison of Additional file 2: Movie S1 and Additional file 3: Movie S2, we found that under same experimental conditions the degummed silk gained a largest water droplet of ~ 2. 53 μL volume in 210 s, but the GSF10 fiber could collected ~ 9.87 and ~ 16.70 μL water droplets in 210 s and 330 s, respectively, indicating the high-speed fog collection could be realized by GSF10 fiber (Fig. 5a). Importantly, to evaluate the purity of the collected water, we further tested the pH value and the electrical resistance. As illustrated in Additional file 1: Fig. S3, the pH of the collected water was 7.02, and the electrical resistance was 1.81 MΩ, which is slightly smaller than that of potable bottle water (2.53 MΩ) but still larger than that in some other reports [32]. The neutral pH and high resistance can manifest the high purity of the collected water [33].

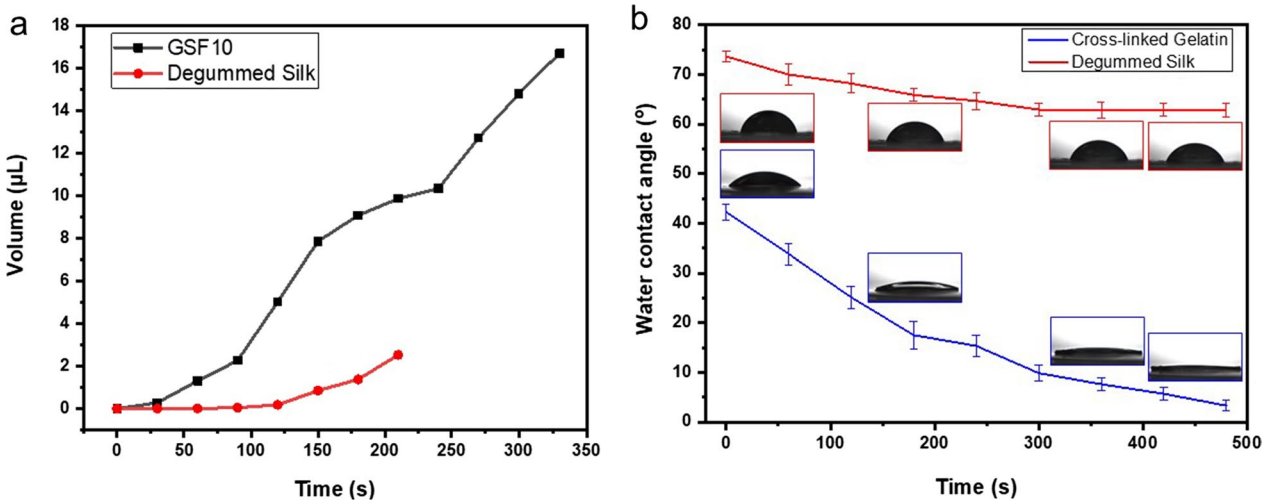

Fig. 5 **a** Water collection performance of GSF10 and uncoated degummed silk. **b** Time-dependent change of the water contact angle of gelatin and gummed silk

For natural SCS, the directional water collection behavior depends on the TCL and the difference in Laplace pressure between the joints and knots region [12]. And for artificial SCS mimicking fibers, it could be controlled by three main factors: chemical gradient induced chemical force (F_C), hysteresis resistance (F_H) and curvature gradient caused Laplace force (F_L) [15, 16]. The equations of these forces of our case were demonstrated in Additional file 1: ES1–3. In brief, the hydrophilicity of gelatin and degummed silk fiber is critical to explain the mechanism of the very fast directional water collection. Therefore, we tested the water contact angles (CAs) of the gelatin film and degummed silk fibroin film. As illustrated in Fig. 5b and Additional file 1: Fig. S4, the initial CA of gelatin film was 44.23 ± 1.63° and it showed a dramatically decreasing trend over time. After 3 min, the CA reduced to 17.57 ± 2.77°. More importantly, after 6 min, it was only around 8.80 ± 1.23°, which means that the water immersed gelatin became a superhydrophilic material [34, 35]. This is because that gelatin could absorb water and be wetted by water very quickly. However, the initial, 3 min and 6 min CAs of degummed silk fibroin films were 73.63 ± 1.12°, 65.87 ± 1.23° and 62.90 ± 1.19°, respectively. It is clear that gelatin is more hydrophilic than degummed silk. Moreover, the superhydrophilic wetted spindle knots region will enlarge the F_C to the knots direction. At the same time, a large F_H will occur because of the rougher surface of knots, making it hard to drive drops away from the knots. Additionally, in current study, F_L of drops on the knots is always ≥ 0 due to the $R_{J'}$ cannot be larger than $R_{K'}$ on the spindle shape knots. Consequently, driven by the combined action of the above three factors, the tiny droplets were motivated toward the hydrophilic knots region and middle drops at a high velocity.

The TCL of water droplets has a significant influence on the threshold droplets volume hanging on the fibers. The TCL could be described as:

$$L = 2m + \pi(b1 + b2) \quad (1)$$

where, as displayed in Additional file 1: Fig. S4, m is the contact length between the fiber and droplets, and b1/b2 represent the diameter of the knots[36]. For GSF10, m is ~ 711.0 μm and the diameter of the knots (b1 and b2) is ~ 78.1 μm. So the theoretical TCL is calculated to be ~ 1.9 cm. However, when water drops appeared on gelatin spindle knots surface, water molecules will enter the knots and the gelatin knots will undergo an obvious swelling and became more hydrophilic simultaneously. As sketched in Additional file 1: Fig. S5a & b, after swelling, the height of the knots (b1' and b2') indicated a ~ 30% enhancement to ~ 101.0 μm, resulting in a larger actual TCL (~ 2059 μm). The volume of a typical knot increased from 0.34 to 0.56 nL. Moreover, the swelling behavior of spindle knots will affect the curvature vale (κ) of the knots. According to previous reports, the curvature of the knots could be defined as κ = tan α = (H − d)/L (α = the semi-axis angle; H = the hump of height; d = the diameter of the fiber; L = the length of hump) [22, 23]. After swelling, the κ increased from 0.36 to 0.52. The swelling induced larger TCL and κ were conducive to sustain bigger drops and speed up the directional collection [18]. Meanwhile, larger surface area of the spindle knots could bring more spots for water collection [37]. A microscope with a digital camera was employed to investigate the swelling and shrinkage behavior of gelatin knots. As displayed in Additional file 4: Movie S3 and Additional file 5: Movie S4, when immersed in water, the knot was observed to swell very quickly due to the high hydrophilicity of the gelatin. After removing the water, the fast dehydration induced a visible volume shrinkage and recovered its original shape eventually. Even after being immersed in water for seven days, the crosslinked gelatin knots can still work well (Additional file 1: Fig. S6a). Meanwhile, Wet/Dry cyclic water collection experiment (one cycle was 12-h water collection and 12-h drying) showed that the water collection ability was almost stable after 7 cycles (Additional file 1: Fig. S6b). This smart behavior of the GSF is similar to the natural SCS when subjected to humid area [21].

To study the fog collection procedure, a typical directional water collection process was observed and recorded in Fig. 6 and Additional file 6: Movie S5. In the high humidity (~ 95% RH) environment subjected the fiber with spindle-knots, and then small water droplets condensed on the surface of both the knots and joints parts. Subsequently, due to the surface energy gradient between these two parts and the roughness of the spindle knots, most droplets were driven toward the knots quickly and then coalesced into bigger droplets. Other tiny water droplets moved to the middle area of the joints between any two knots and constructed larger middle droplets. These middle droplets could act as temporary knots which may help accelerate the accumulation of fog. As the diameter of droplets increased continuously, the middle drops would contact the large knot drops, and then coalesced larger drops appeared between two knots. The continuous occurrence of this process eventually led to huge water droplets gathering between the knots, facilitating the fast directional fog collection.

Additionally, the comparison of the directional water collection ability of gelatin coated degummed silk (GSF), eMaSp2 coated degummed silk (eMaSp2 on Silk), and nylon based fibers coated by PMMA (PMMA on Nylon), PDMS (PDMS on Nylon), and PVDF (PVDF on Nylon) is shown in Fig. 7. Compared to other

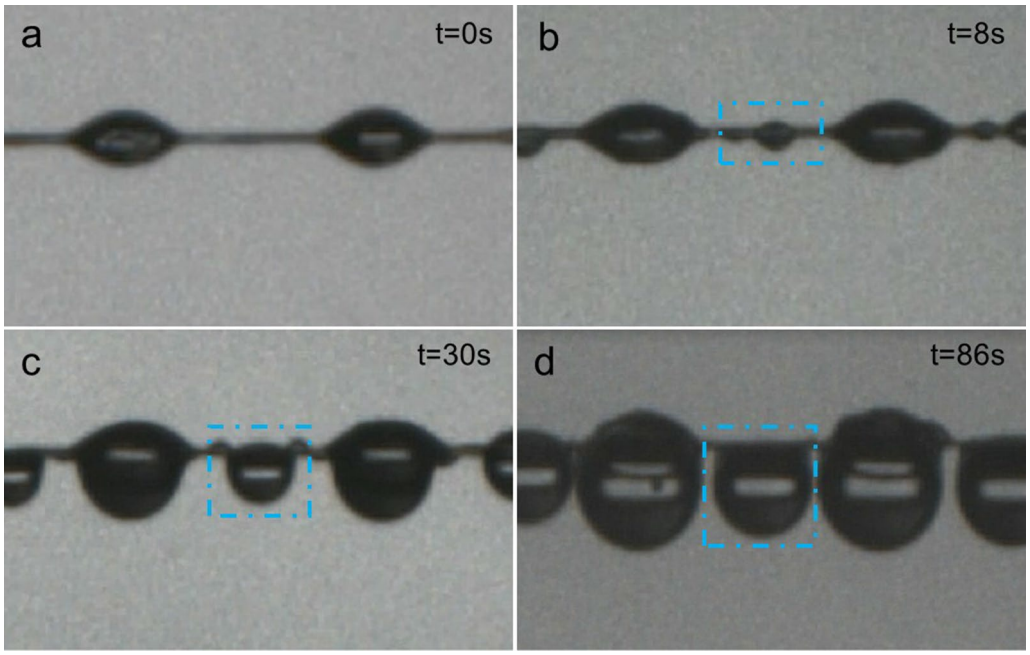

Fig. 6 Digital photos showed the formation of middle drops at different time of pionts (**a** 0 s; **b** 8 s; **c** 30 s; **d** 86 s)

artificial fibers, the GSF10 could sustain largest water droplets (~ 16.70 μL) between two knots with moderate TCL (~ 2 cm), which is larger than all Nylon-based SCS mimicking fibers and more than two times as the eMaSp2 on Silk. Even the PVDF on Nylon fiber with quite bigger size knots (200 μm knot height, 666 μm knot length and 98 μm fiber diameter), which claimed to harvest largest volume of water droplet (~ 13.10 μL), can hardly reach the water collection capability of GSF10 (see Fig. 7a). To be precise, the volume-to-TCL index (VTTI) was calculated to demonstrate the water collection effiency of the fibers. As shown in Fig. 7b and Additional file 1: Table S1, GSF10 fiber displayed highest VTTI among all the reported fibers, owing to the superhydrophilicity and roughness of the gelatin spindle knots. Besides, the the weight of per unit of the GSF (1.59 μg) is only ~ 2% of PVDF on Nylon fiber (63.7 μg). The relationship between maximal volume and volume-to-mass index (VTMI) was summrized in Fig. 7c. Although the VTMI of GSF10 is less than eMaSp2 on Silk fiber, but it is larger than other fibers and GSF can hold much bigger water droplets than eMaSp2 on Silk fiber. In practical application, longer TCL useally means the longer length of the fiber. Therefore, in a given space with specific length, fiber with larger VTTI could gain more water and subsequently enhance the space utilization rate (Fig. 7d). More importantly, to evaluate the scability of this novel fiber, the cost to produce one kilogram (~ 6.7×10^6 m) fiber was estimated to be approximately 1.25 USD (see Additional file 1), which is ecnomical and has the promise of being promoted in reality.

4 Conclusions

In conclusion, we have fabricated a series of SCS mimicking fibers by a facile dip-coating strategy toward high efficiency fog collection. The superhydrophilic and rough spindle knots constructed by crosslinked gelatin demonstrated unparalleled directional water collection speed and performance for harvesting ~ 16.70 μL water within 330 s. The threshold water droplet volme of this fiber is larger than PVDF coated Nylon fiber that reported to collect largest water droplet (13.10 μL) ever, but the TCL and mass of per unit of GSF10 fiber are only 74% and 2% of PVDF on Nylon fiber. The fiber also displayed a highest fog collection effeciency aomong all coated nylon fibers as well as the eMaSp2 spidroin coated degummed silk in terms of VTTI. This ultra-high fog collection ability and efficiency are attributed to the synergistic effect of the superhydrophilicity, surface roughness and volume swelling of the gelatin spindle knots and the small diameter of degummed silk. The novel fibers exbited good mechanical property even after one year storage. The apllication of gelatin in this work can not only provide a green and cost-effective strategy toward the design and fabrication of eco-friendly fog collection device with scalable potential, but broaden the application of the widely available biomass—gelatin and silkworm silk.

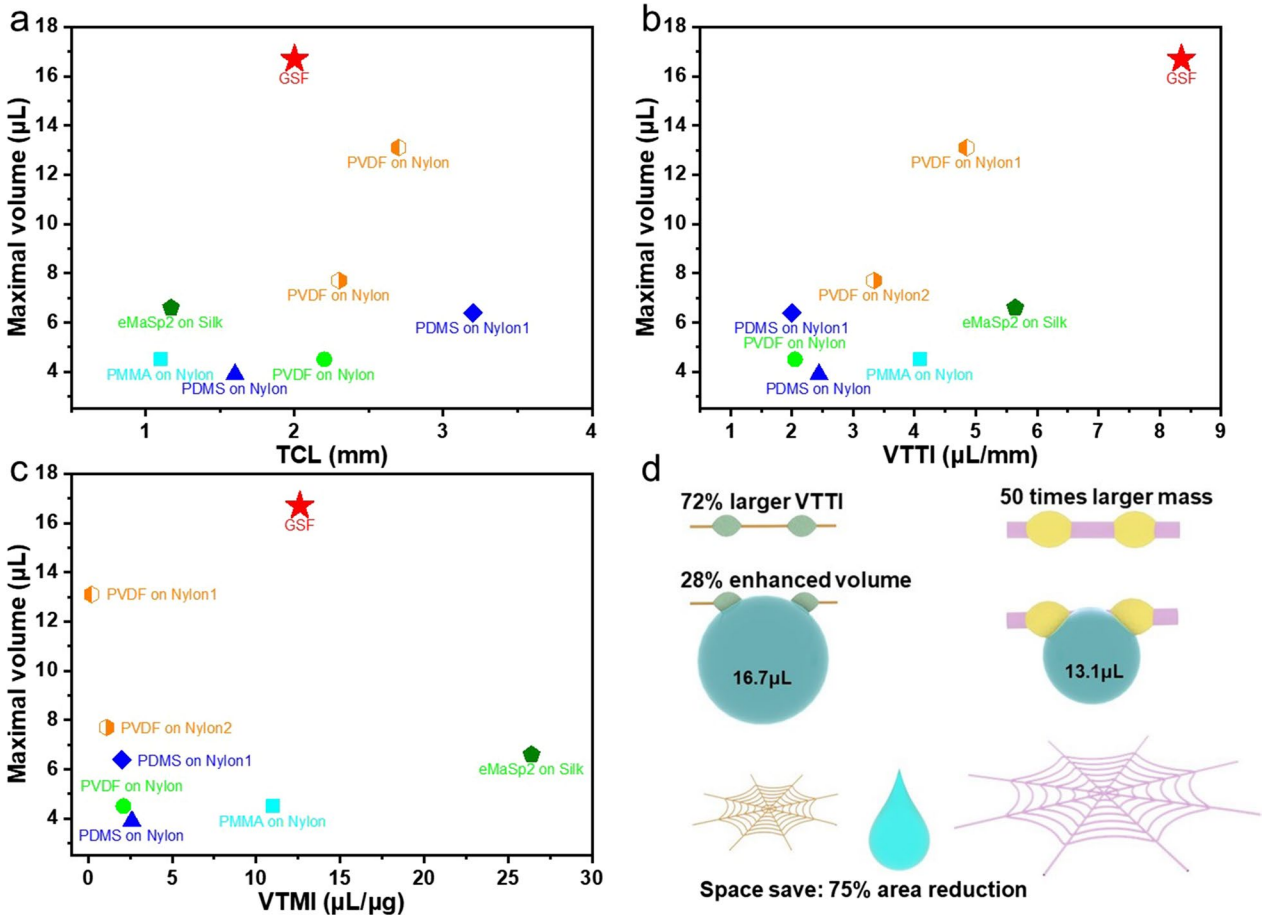

Fig. 7 Comparison of fog collection performance. **a** Maximal volume of droplets collected by different SCS mimicing fibers with various TCLs. **b** Maximal volume versus volume-to-TCL index (VTTI) for GSF10 and previous reported fibers. **c** Maximal volume versus volume-to-mass index (VTMI) for GSF10 and previous reported fibers [23]. **d** Schematic picture showing comparison of water collection performance between GSF10 and the best existing polymer fiber regarding the efficiency, VTTI and mass

Abbreviations

SCS	Spider-capture-silk
GSF	Gelatin on silk fiber
TCL	Three phase contact line
PVA	Poly(vinyl alcohol)
PMMA	Polymethyl methacrylate
PS	Polystyrene
PVDF	Polyvinylidene difluoride
VTTI	Volume-to-TCL index
VTMI	Volume-to-mass index
HFIP	1, 1, 1, 3, 3, 3-Hexafluoroisopropanol
SEM	Scanning electron microscope

Supplementary Information

The online version contains supplementary material available at https://doi.org/10.1186/s42825-023-00112-y.

Additional file 1. Fig. S1 SEM image of fibers coated by 8% a) and 12% b) gelatin/HFIP solution; c) Uncross-linked gelatin knots after 2 hours application. **Fig. S2** FTIR spectra of degummed silk and GSF10. **Fig. S3** pH and electrical resistance tests of the collected water. **Fig. S4** Images show the water contact angle of gelatin and silk fibroin films and their changes with time. a) Gelatin film. b) Silk fibroin film. **Fig. S5** Gelatin knots before a) and after b) swelling. **Fig. S6** a) Time-dependent water collection performance of GSF10. b) Wet/Dry cyclic water collection performance of GSF10.

Additional file 2. Movie S1 Water collection process of degummed silk.

Additional file 3. Movie S2 Water collection process of GSF10.

Additional file 4. Movie S3 Water absorption and volume swell of a gelatin knot.

Additional file 5. Movie S4 Dehydration and volume shrinkage of a gelatin knot.

Additional file 6. Movie S5 A typical directional water collection process.

Acknowledgements
We thank Mr. Hao Luo and Mr. Pengfei Tan for their help in water collection experiment.

Author contributions
YJ and LT conceived the idea. YJ conducted the experiment with the help of CW. YJ analyzed the data with the help of SS and MC. YJ drafted the manuscript. JH and YJ revised the manuscript. All authors read and approved the final manuscript.

Funding
The National Natural Science Foundation of China (Nos. 52073186, 52073241); State Key Laboratory of Polymer Materials Engineering (sklpme2021-3–01); Funding of Engineering Characteristic Team, Sichuan University (2020SCUNG122); Hong Kong General Research Fund (15201719); the Guangdong Basic and Applied Basic Research Foundation, Shenzhen Joint Fund, Youth Fund Project 2019 (2019A1515111207).

Availability of data and materials
All data generated or analysed during this study are included in this published article, and its supplementary information files.

Declarations

Competing interests
The authors declare that they have no competing interests.

Author details
[1]College of Biomass Science and Engineering, Key Laboratory of Leather Chemistry and Engineering of Ministry of Education, Sichuan University, Chengdu 610065, China. [2]Department of Textile and Fibre Engineering, Indian Institute of Technology, Delhi, New Delhi 110016, India. [3]Department of Biomedical Engineering, City University of Hong Kong, Kowloon 999077, Hong Kong SAR, China. [4]Shenzhen Bay Laboratory, Shenzhen 518132, China. [5]Key Laboratory of Biochip Technology, Shenzhen Biotech and Health Centre, City University of Hong Kong Shenzhen Research Institute, Shenzhen 518057, China. [6]State Key Laboratory of Polymer Materials Engineering, Sichuan University, Chengdu 610065, China. [7]City University of Hong Kong Shenzhen Research Institute, Shenzhen 518057, China.

Received: 24 October 2022 Revised: 3 January 2023 Accepted: 5 January 2023
Published online: 03 February 2023

References

1. Vörösmarty CJ, Green P, Salisbury J, Lammers RB. Global water resources: vulnerability from climate change and population growth. Science. 2000;289(5477):284–8.
2. Ma T, Sun S, Fu G, Hall JW, Ni Y, He L, et al. Pollution exacerbates China's water scarcity and its regional inequality. Nat Commun. 2020;11(1):1–9.
3. Klemm O, Schemenauer RS, Lummerich A, Cereceda P, Marzol V, Corell D, et al. Fog as a fresh-water resource: overview and perspectives. Ambio. 2012;41(3):221–34.
4. Wang H, Wang DT, Zhang XY, Zhang ZZ. Modified PDMS with inserted hydrophilic particles for water harvesting. Compos Sci Technol. 2021;213:108954.
5. Gurera D, Bhushan B. Passive water harvesting by desert plants and animals: lessons from nature. Phil Trans R Soc A. 2020;378(2167):20190444.
6. Liu K, Jiang L. Multifunctional integration: from biological to bio-inspired materials. ACS Nano. 2011;5(9):6786–90.
7. Nørgaard T, Dacke M. Fog-basking behaviour and water collection efficiency in Namib Desert Darkling beetles. Front Zool. 2010;7(1):1–8.
8. Zhu H, Cai S, Zhou J, Li S, Wang D, Zhu J, et al. Integration of water collection and purification on cactus-and beetle-inspired eco-friendly superwettable materials. Water Res. 2021;206:117759.
9. Zhu H, Duan R, Wang X, Yang J, Wang J, Huang Y, et al. Prewetting dichloromethane induced aqueous solution adhered on Cassie superhydrophobic substrates to fabricate efficient fog-harvesting materials inspired by Namib Desert beetles and mussels. Nanoscale. 2018;10(27):13045–54.
10. Lee A, Moon M-W, Lim H, Kim W-D, Kim H-Y. Water harvest via dewing. Langmuir. 2012;28(27):10183–91.
11. Comanns P, Esser FJ, Kappel PH, Baumgartner W, Shaw J, Withers PC. Adsorption and movement of water by skin of the Australian thorny devil (Agamidae: Moloch horridus). R Soc Open Sci. 2017;4(9):170591.
12. Zheng Y, Bai H, Huang Z, Tian X, Nie F-Q, Zhao Y, et al. Directional water collection on wetted spider silk. Nature. 2010;463(7281):640–3.
13. Shi R, Tian Y, Wang L. Bioinspired fibers with controlled wettability: from spinning to application. ACS Nano. 2021;15(5):7907–30.
14. Liu H, Wang Y, Yin W, Yuan H, Guo T, Meng T. Highly efficient water harvesting of bioinspired spindle-knotted microfibers with continuous hollow channels. J Mater Chem A. 2022. https://doi.org/10.1039/D2TA00242F.
15. Chen W, Guo Z. Hierarchical fibers for water collection inspired by spider silk. Nanoscale. 2019;11(33):15448–63.
16. Bai H, Tian X, Zheng Y, Ju J, Zhao Y, Jiang L. Direction controlled driving of tiny water drops on bioinspired artificial spider silks. Adv Mater. 2010;22(48):5521–5.
17. Bai H, Ju J, Sun R, Chen Y, Zheng Y, Jiang L. Controlled fabrication and water collection ability of bioinspired artificial spider silks. Adv Mater. 2011;23(32):3708–11.
18. Tian X, Chen Y, Zheng Y, Bai H, Jiang L. Controlling water capture of bioinspired fibers with hump structures. Adv Mater. 2011;23(46):5486–91.
19. Hou Y, Chen Y, Xue Y, Wang L, Zheng Y, Jiang L. Stronger water hanging ability and higher water collection efficiency of bioinspired fiber with multi-gradient and multi-scale spindle knots. Soft Matter. 2012;8(44):11236–9.
20. Tian Y, Zhu P, Tang X, Zhou C, Wang J, Kong T, et al. Large-scale water collection of bioinspired cavity-microfibers. Nat Commun. 2017;8(1):1–9.
21. Tian X, Bai H, Zheng Y, Jiang L. Bio-inspired heterostructured bead-on-string fibers that respond to environmental wetting. Adv Func Mater. 2011;21(8):1398–402.
22. Chen Y, Li D, Wang T, Zheng Y. Orientation-Induced effects of water harvesting on humps-on-strings of bioinspired fibers. Sci Rep. 2016;6(1):1–7.
23. Venkatesan H, Chen J, Liu H, Liu W, Hu J. A spider-capture-silk-like fiber with extremely high-volume directional water collection. Adv Func Mater. 2020;30(30):2002437.
24. Mitura S, Sionkowska A, Jaiswal A. Biopolymers for hydrogels in cosmetics. J Mater Sci - Mater Med. 2020;31(6):1–14.
25. Samborska K, Boostani S, Geranpour M, Hosseini H, Dima C, Khoshnoudi-Nia S, et al. Green biopolymers from by-products as wall materials for spray drying microencapsulation of phytochemicals. Trends Food Sci Technol. 2021. https://doi.org/10.1016/j.tifs.2021.01.008.
26. Collin MA, Clarke TH, Ayoub NA, Hayashi CY. Evidence from multiple species that spider silk glue component ASG2 is a spidroin. Sci Rep. 2016;6(1):1–12.
27. Pal A, Bajpai J, Bajpai A. Easy fabrication and characterization of gelatin nanocarriers and in vitro investigation of swelling controlled release dynamics of paclitaxel. Polym Bull. 2018;75(10):4691–711.
28. Liu X, Shi L, Wan X, Dai B, Chen Y, Wang S. Recent progress of spider-silk-inspired adhesive materials. ACS Mater Lett. 2021;3(10):1453–67.
29. Rockwood DN, Preda RC, Yücel T, Wang X, Lovett ML, Kaplan DL. Materials fabrication from Bombyx mori silk fibroin. Nat Protoc. 2011;6(10):1612–31.
30. Liu M, Wang S, Jiang L. Nature-inspired superwettability systems. Nat Rev Mater. 2017;2(7):1–17.
31. Kim HJ, Kim MK, Lee KH, Nho SK, Han MS, Um IC. Effect of degumming methods on structural characteristics and properties of regenerated silk. Int J Biol Macromol. 2017;104:294–302.
32. Gong F, Li H, Zhou Q, Wang M, Wang W, Lv Y, et al. Agricultural waste-derived moisture-absorber for all-weather atmospheric water collection and electricity generation. Nano Energy. 2020;74:104922.
33. Zhao F, Zhou X, Shi Y, Qian X, Alexander M, Zhao X, et al. Highly efficient solar vapour generation via hierarchically nanostructured gels. Nat Nanotechnol. 2018;13(6):489–95.
34. Chaudhary JP, Nataraj SK, Gogda A, Meena R. Bio-based superhydrophilic foam membranes for sustainable oil–water separation. Green Chem. 2014;16(10):4552–8.
35. Talukder ME, Hasan K, Wang J, Yao J, Li C, Song H. Novel fibrin functionalized multilayered electrospun nanofiber membrane for burn wound treatment. J Mater Sci. 2021;56(22):12814–34.
36. Hou Y, Chen Y, Xue Y, Zheng Y, Jiang L. Water collection behavior and hanging ability of bioinspired fiber. Langmuir. 2012;28(10):4737–43.
37. Wang S, Feng S, Hou Y, Zheng Y. Controlling of water collection ability by an elasticity-regulated bioinspired fiber. Macromol Rapid Commun. 2015;36(5):459–64.

Publisher's Note